Supplementary Material

Enhanced near-infrared light-induced photoresponse via transition of monocrystalline phase and surface reconstruction

Hong Jia (贾 红)[1*,†], Hongming Jiang (蒋洪明)[1,2,†], Yuping Zhang (张瑜萍)[1], Shuxu Hua (华淑旭)[1], Qing Liu (刘 青)[1], Yuquan Yuan (袁玉全)[2], Yanfei Hu (胡燕飞)[3], Feng Peng (彭 枫)[1***], and Xiaofeng Liu (刘小峰)[4****]**

[1] College of Physics and Electronic Information & Key Laboratory of Electromagnetic Transformation and Detection of Henan province, Luoyang Normal University, Luoyang 471934, China.
[2] School of Physics and Electronic Engineering, Sichuan University of Science & Engineering, Zigong 643000, China.
[3] Department of Applied Physics, Chengdu University of Technology, Chengdu, People's Republic of China.
[4] School of Materials Science and Engineering, Zhejiang University, Hangzhou 310027, China.
*Corresponding author: jiahong517@aliyun.com
**Corresponding author: yanfeihususe@suse.edu.cn
***Corresponding author: fpeng@lynu.edu.cn
****Corresponding author: xfliu@zju.edu.cn
[†]These authors contributed equally to this work.

Structural and morphological characteristics

The phase structure of the Gd_2O_3: Er^{3+}, M^+ (M=Na, K, Cs) phosphor samples was determined by X-ray diffraction (XRD) measurements. Fig. S1(a) displays the XRD patterns of Gd_2O_3 phosphors doped with Er^{3+} concentrations of 1, 3, 5, 7, 10, 12, and 15 mol%. All diffraction peaks correspond well to the cubic phase G_2O_3 (JCPDS No. 12-0797) with the space group *Ia-3*. With a closer observation, a weak peak is shown at 2θ-32 °, which can be attributed to the monoclinic phase of Gd_2O_3, which can be transformed into a cubic phase by increasing the annealing temperature (Fig. S1(d)) [1]. For the overall right shift of the main peak of the samples, this is related to the lattice shrinkage caused by the replacement of the larger Gd^{3+} ion (0.938 Å) by the smaller Er^{3+}(ion radius (0.89 Å)) [2]. Fig. S1(b) showed the XRD patterns of Gd_2O_3: 3% Er^{3+}, $x$$Na^+$ (x=1, 3, 5, 7, 10, 12 mol%) phosphor. It can be found that the introduction of Na^+ ions does not generate other impurity phases, but the peak width is significantly narrowed. The evolution of sharp diffraction peaks indicates a significant increase in crystallinity after the introduction of Na^+ ions, which may be related to the lower phase formation temperature caused by the low melting point of the Na^+ precursor [3]. Meanwhile, the overall diffraction peak shifts to a smaller angle for the samples of Gd_2O_3: 3% Er^{3+} with the increase of Na^+ doping concentration (Fig. S2, Supporting Information). This is because the alkali ions (i.e., Na^+) enter into the interstitial sites, which leads to the expansion of the host lattice. In addition, the XRD patterns of K^+ and Cs^+ ions introduced into Gd_2O_3: 3% Er^{3+} phosphors were also recorded. As shown in Fig. S1(c, f), the increase of the absolute height of the diffraction peak and the decrease of the peak width again prove that the introduction of alkali metals contributes to the improved crystallinity of phosphors. The lattice parameters of Gd_2O_3, Gd_2O_3: 3% Er^{3+}, and Gd_2O_3: 3% Er^{3+}, N (N=10% Na^+, 7% K^+ and 3% Cs^+) were obtained by Rietveld refinement, which revealed the effect of the introduction of different alkali metal elements on the lattice parameters and cell volume. As shown in Table S1 (Supporting Information), the lattice parameters show the trend of first decreasing and then increasing with the addition of Er^{3+} and alkali metal ions. This result proves again that the lattice of Gd_2O_3: 3% Er^{3+}, M^+ (M= Na, K, and Cs) phosphors contracts first and then expands with the addition of doping ion

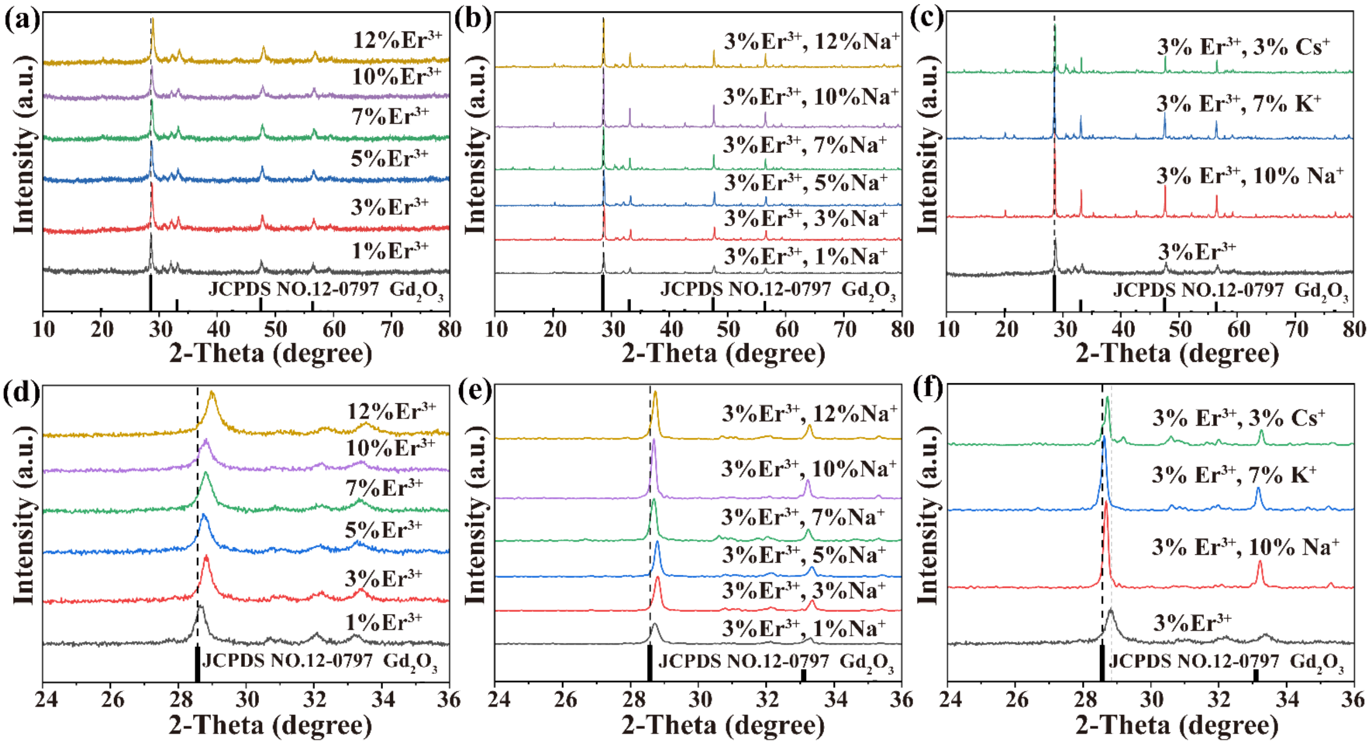

Fig. S1. (a)-(c) XRD patterns and (d)-(f) enlarged regions (24–36 °) of Gd_2O_3: x% Er^{3+} + y% M^+ (x, y =1, 3, 5, 7, 10, 12, 15; M= Na, K, Cs).

Table S1. Lattice parameters of Gd_2O_3, Gd_2O_3: 3%Er^{3+} and Gd_2O_3: 3%Er^{3+}, N (N= 10%Na^+, 7%K^+ and 3%Cs^+) obtained by Rietveld refinement.

Samples	*a* (Å)	*b* (Å)	*c* (Å)	Space groups	Volume ($Å^3$)
Gd_2O_3	10.813	10.813	10.813	Ia-3 (206)	1264.27
Gd_2O_3: 3%Er^{3+}	10.759	10.759	10.759	Ia-3 (206)	1245.60
Gd_2O_3: 3%Er^{3+}, 10%Na^+	10.788	10.788	10.788	Ia-3 (206)	1255.52
Gd_2O_3: 3%Er^{3+}, 7%K^+	10.794	10.794	10.794	Ia-3 (206)	1257.93
Gd_2O_3: 3%Er^{3+}, 3%Cs^+	10.778	10.778	10.778	Ia-3 (206)	1252.19

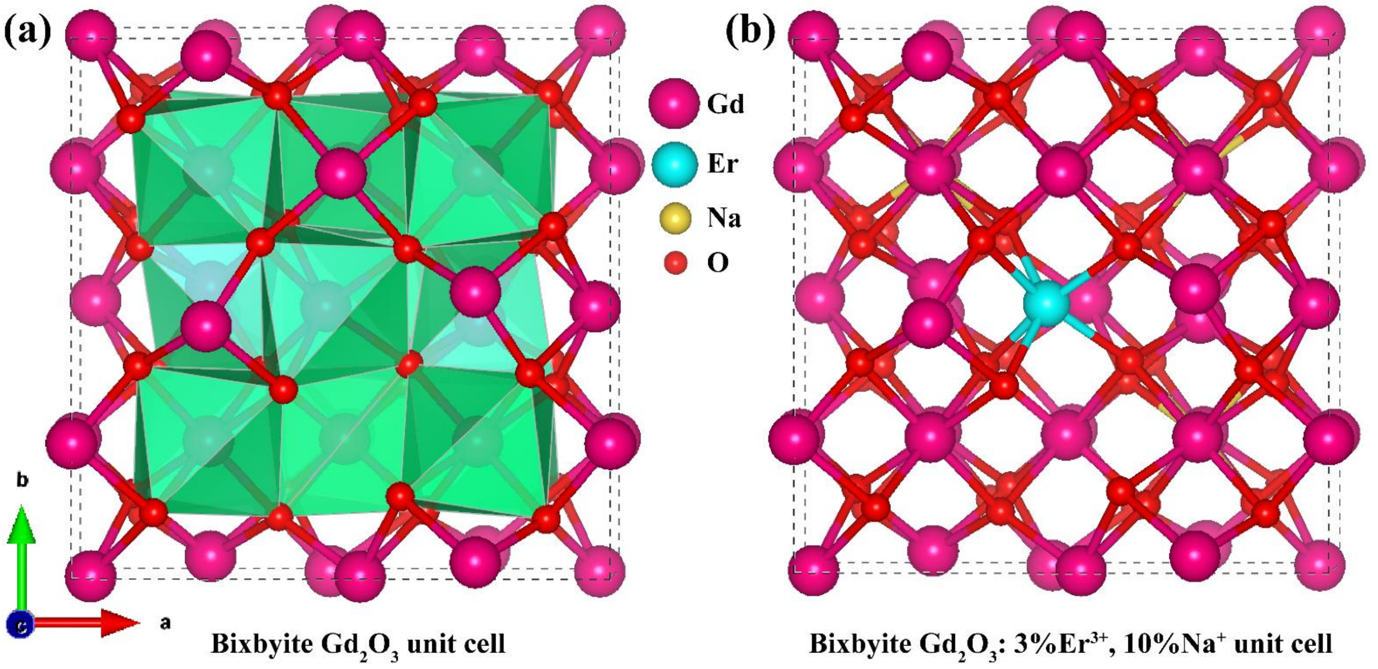

Fig. S2. (a) Crystal structure of the Gd_2O_3. (b) Possible crystal structure of Er, Na co-doped Gd_2O_3.

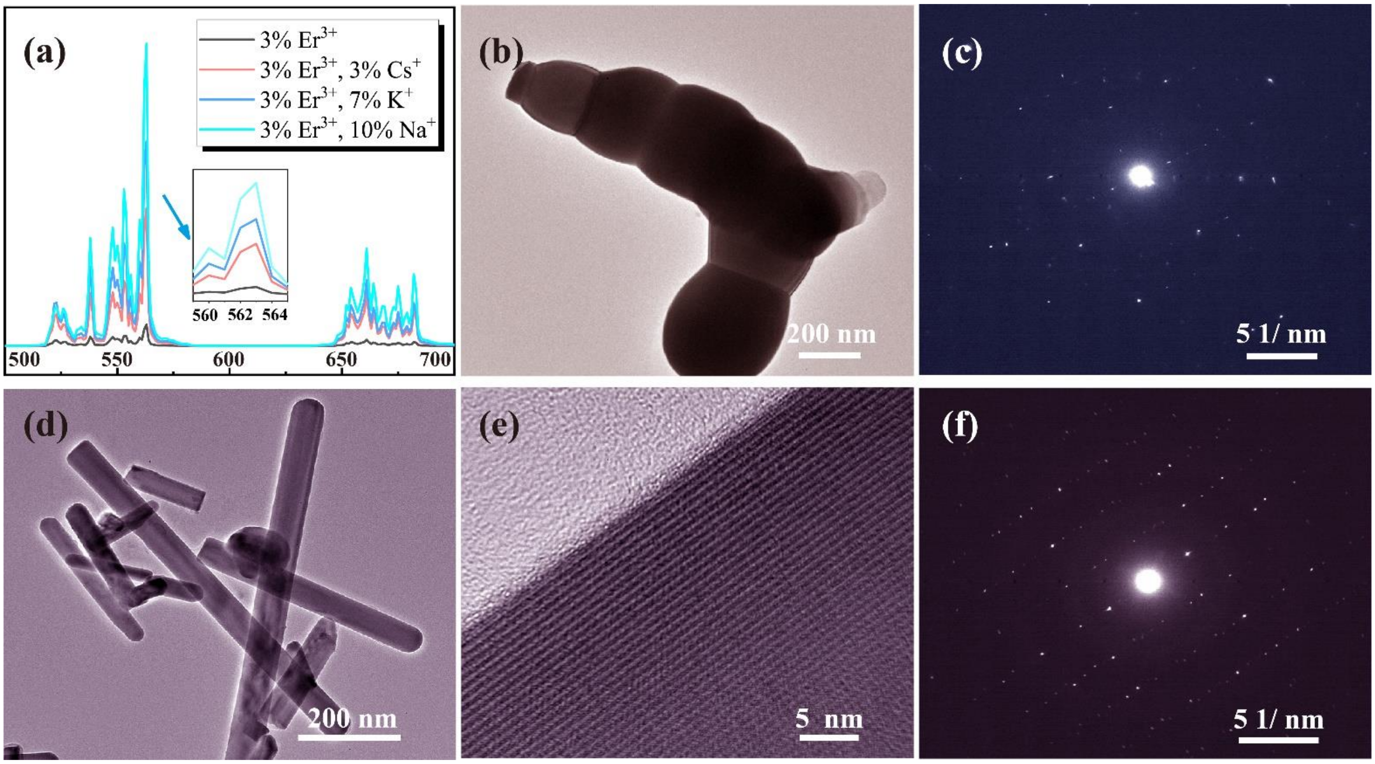

Fig. S3. (a) UC spectral of the Gd_2O_3: 3%Er^{3+} and Gd_2O_3: 3%Er^{3+}, N (N= 10%Na^+, 7%K^+ and 3%Cs^+) phosphors recorded after stored in ambient condition for 60 days. (b) TEM and (c) SAED of Gd_2O_3: 3%Er^{3+}, 7%K^+ phosphors. (d) TEM, (e) HRTEM and (f) SAED of Gd_2O_3: 3%Er^{3+}, 3%Cs^+ phosphors.

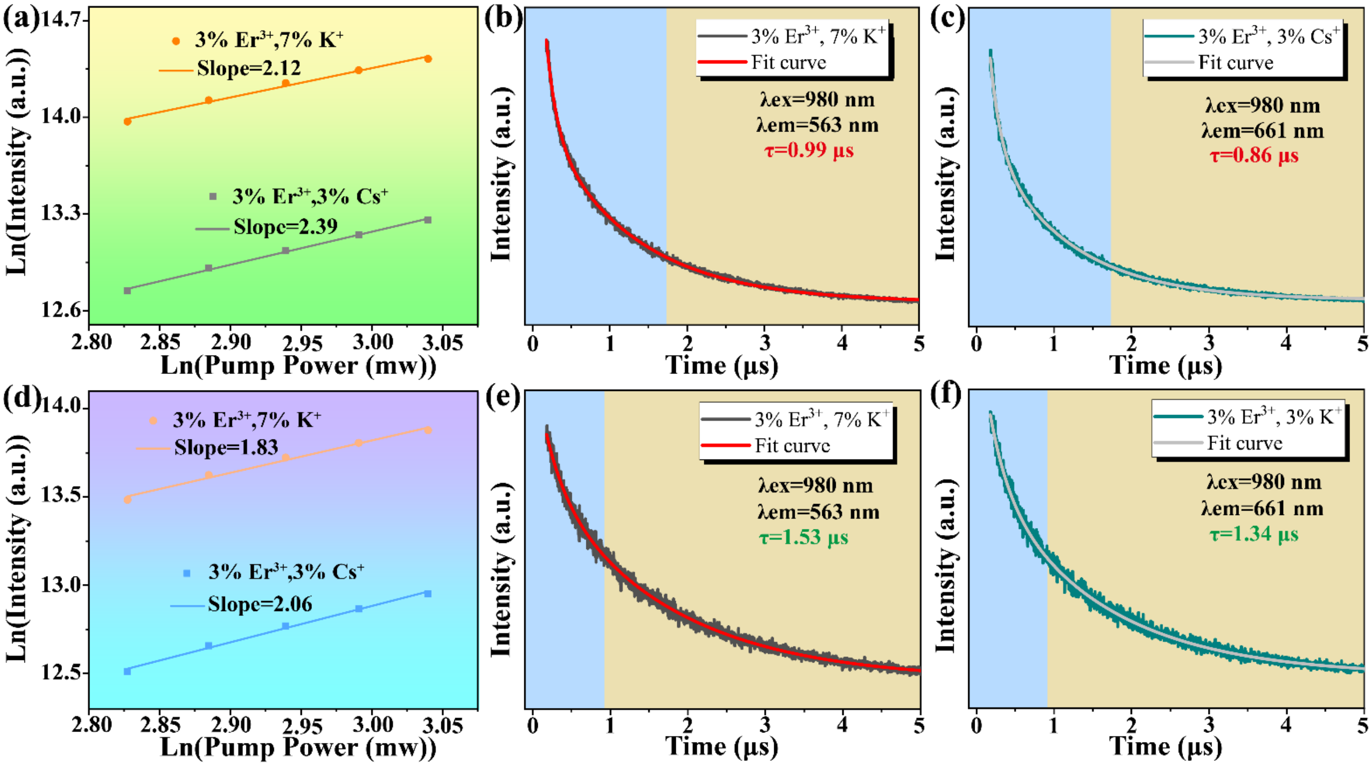

Fig. S4. (a), (d) The power-dependent emission intensity of Gd_2O_3: 3% Er^{3+}, M^+ (M = K, Cs) phosphors. (b), (c) and (e), (f) Emission decay curves of Gd_2O_3: 3% Er^{3+}, 7% K^+ and Gd_2O_3: 3% Er^{3+}, 3% Cs^+ phosphors at 563 and 661 nm (980 nm excitation).

References

1. R. Priya, O.P. Pandey, S.J. Dhoble, "Review on the synthesis, structural and photo-physical properties of Gd_2O_3 phosphors for various luminescent applications," Opt Laser Technol **135**, 106663 (2021).
2. B.R.D. Shannon, "Revised Effective Ionic Radii and Systematic Studies of Interatomie Distances in Halides and Chaleogenides," Acta Crystallogr A **32**, 751 (1976).
3. X. Yang, M. Liu, J. Liu, Y. Xia, W. Ji, Z. Li, J. Chen, L. Liu, L. Hao, B. Dong, S. Agathopoulos, X. Xu, "Mechanism of upconversion luminescence enhancement in Yb^{3+}/Er^{3+} co-doped Y_2O_3 through Li^+ incorporation," Phys. Chem. Chem. Phys. **22**, 2819 (2020).